 doi:10.20944/preprints202012.0354.v1

Discovery and Optimization of Selective Inhibitors of Meprin α (Part I)

Shurong Hou[1,3] Juan Diez[2], Chao Wang[3], Christoph Becker-Pauly[4], Gregg B. Fields[5], Thomas Bannister[3], Timothy P. Spicer[1,3] Louis D. Scampavia[1,3] and Dmitriy Minond[2,6]

[1] - The Scripps Research Molecular Screening Center, Department of Molecular Medicine, Scripps Research, Jupiter, Florida 33458

[2] - Rumbaugh-Goodwin Institute for Cancer Research, Nova Southeastern University, 3321 College Avenue, CCR r.605, Fort Lauderdale, FL 33314

[3] - Department of Molecular Medicine, Scripps Research, Jupiter, Florida 33458

[4] - University of Kiel, Institute of Biochemistry, Unit for Degradomics of the Protease Web, Rudolf-Höber-Str.1, 24118 Kiel, Germany

[5] - Department of Chemistry & Biochemistry and I-HEALTH, Florida Atlantic University, 5353 Parkside Drive, Jupiter, FL 33458

[6] - Dr. Kiran C. Patel College of Allopathic Medicine, Nova Southeastern University, 3301 College Avenue, Fort Lauderdale, FL 33314

*Correspondence to: Dmitriy Minond, Rumbaugh-Goodwin Institute for Cancer Research, Nova Southeastern University, 3321 College Avenue, CCR r.605, Fort Lauderdale, FL 33314, dminond@nova.edu;

Short title: Selective inhibitors of meprin α

Subject category: Enzymatic assays

KEYWORDS: meprin α, meprin β, zinc metalloproteinase, uHTS.

 doi:10.20944/preprints202012.0354.v1

ABSTRACT

Meprin α and β are zinc-dependent proteinases implicated in multiple diseases including cancers, fibrosis, and Alzheimer's. However, until recently, only a few inhibitors of either meprin were reported and no inhibitors are in pre-clinical development. Moreover, inhibitors of other metzincins developed in previous years are not effective in inhibiting meprins suggesting the need for *de novo* discovery effort. To address the paucity of tractable meprin inhibitors we developed ultra-high throughput assays and conducted parallel screening of >650,000 compounds against each meprin. As a result of this effort, we identified 5 selective meprin α hits belonging to three different chemotypes (triazole-hydroxyacetamides, sulfonamide-hydroxypropanamides, and phenoxy-hydroxyacetamides). These hits demonstrated a nanomolar to micromolar inhibitory activity against meprin α with low cytotoxicity and >30-fold selectivity against meprin β and other related metzincincs. These are the most selective inhibitors of meprin α to date.

Preprints (www.preprints.org) | NOT PEER-REVIEWED | Posted: 14 December 2020 doi:10.20944/preprints202012.0354.v1

INTRODUCTION

Meprin α and meprin β are zinc-dependent proteinases implicated in multiple diseases including cancers [1], fibrosis [2, 3], and Alzheimer's [4, 5]. Due to the relatively recent discovery of meprins' involvement in pathologic conditions there are very few reports of inhibitors discovery efforts for these enzymes. Kruse *et al*., [6] reported several known metzincin inhibitors that are capable of inhibiting meprins with some degree of selectivity. However, these inhibitors were not selective for other metzincins, which made their utilization for studying the roles of meprins in various diseases difficult. Our group had reported the first low nanomolar meprin β inhibitors, NFF449 and PPNDS (Fig. 1, K_i = 22 nM and 8 nM, respectively), with ~100-fold selectivity against meprin α and good selectivity against adamalysins and matrixins [7]. Ramsbeck *et al*., (2017) reported the low nanomolar selective meprin β inhibitor, **11g,** with 46-fold selectivity against meprin α (Fig. 1, IC_{50} = 2,735 nM and 60 nM for meprin α and β, respectively) with good selectivity against adamalysins and matrixins [8]. They also reported improved compounds based on the same scaffold [9] (Fig. 1). The best compounds from this series, **8h** and **8i**, are 27-fold and 15-fold selective against meprin α (IC_{50} = 23 nM and 626 nM for **8h** and 24 nM and 368 nM for **8i**, for meprin β and α, respectively). 200 μM of either inhibitor had only limited effect on MMP and ADAM activity, but IC_{50} values were not reported. Tan *et al*., (2018) reported the first selective inhibitors of meprin α, **10d** and **10e**, with 18- and 19-fold selectivity against meprin β [10] (Fig. 1). Herein we report the results of a large-scale parallel high screening throughput effort to discover novel inhibitors of meprin α and meprin β.

Preprints (www.preprints.org) | NOT PEER-REVIEWED | Posted: 14 December 2020 doi:10.20944/preprints202012.0354.v1

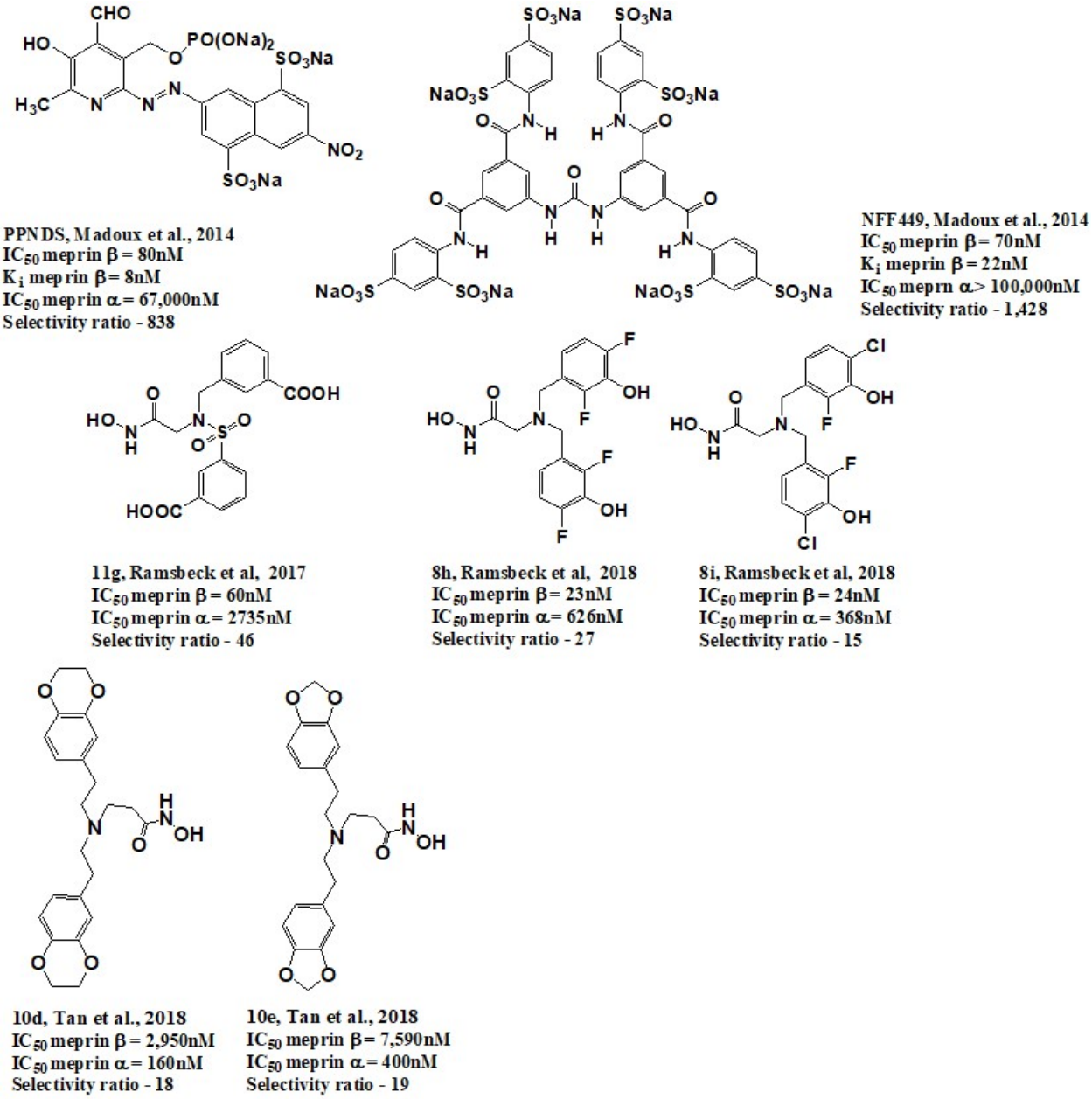

Figure 1. Synthetic selective meprin inhibitors described to date.

RESULTS

Assay miniaturization and optimization in 1,536 well plate format. The meprin α and meprin β assays, which utilize the substrates (Mca)-YVADAPK-(K-ε-Dnp) and (Mca)-EDEDED-(K-ε-

Preprints (www.preprints.org) | NOT PEER-REVIEWED | Posted: 14 December 2020 doi:10.20944/preprints202012.0354.v1

Dnp), respectively, have been described previously [7]. To enable an ultra-high-throughput screening (uHTS) campaign, we proceeded to miniaturize both assays to 1,536 well plate format (wpf). First, we recapitulated the assays in 1,536 well plate using reagents at the same concentrations as in a 384 well plate format assays by scaling the volume down by the factor of 2.5. This resulted in the final volume of the assays of 4 µL. The meprin α assay in 1,536 well plates demonstrated a lower signal-to-basal (S/B) ratio than in 384 well plates (1.85 vs 2.3, respectively), but a better Z' value (0.76 vs 0.6, respectively), suggesting that the assay is very suitable for large-scale HTS [11]. Actinonin's IC_{50} values were within 2-fold of each other (5.7 nM and 11 nM for 1,536 and 384 well plate format, respectively) (Fig. 2A and Table 1).

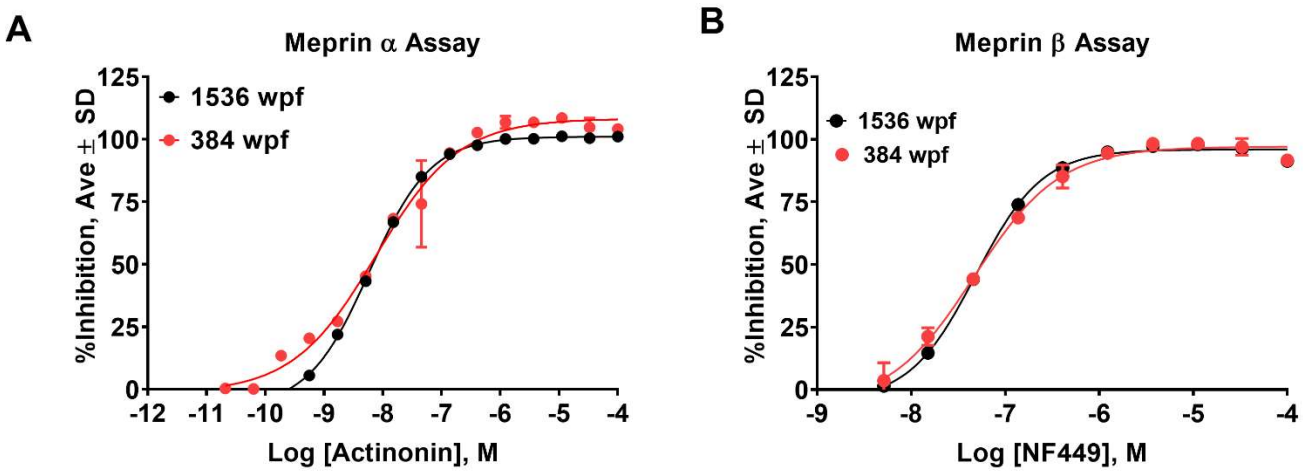

Figure 2. Assay recapitulation in 1,536 well plate format. Concentration response studies in 384 and 1,536 well plate formats show similar potency of pharmacological controls for (A) meprin α (actinonin) and (B) meprin β (NF449) assays. Both assays were performed in triplicate.

Table 1. Comparison of meprin α and meprin β assay parameters in 384 and 1,536 well plate formats.

Assay	S/B	Z'	Actinonin IC_{50}, nM	NFF449 IC_{50}, nM

Preprints (www.preprints.org) | NOT PEER-REVIEWED | Posted: 14 December 2020 doi:10.20944/preprints202012.0354.v1

Meprin α 384 wpf	2.3	0.6	11	>100,000
Meprin α 1,536 wpf	1.85	0.76	5.7	>100,000
Meprin β 384 wpf	4.4	0.9	22,000	53
Meprin β 1,536 wpf	6.9	0.91	9,750	48

Meprin β assay exhibited greater S/B in 1,536 wpf than in 384 wpf (6.9 vs 4.4, respectively), while Z' factor values were identical at 0.9. NFF449 IC_{50} values were 48 nM and 53 nM for 1,536 and 384 wpf, respectively (Fig. 2B and Table 1). Despite excellent Z' values in the 1,536 wpf in both assays, we wanted to ensure an optimal balance between robustness and sensitivity; in particular with meprin α.

First, both assays were run for 180 min at three different enzyme concentrations including the concentrations at which the assays were recapitulated in 1,536 wpf (1.3 nM and 0.05 nM for meprin α and meprin β, respectively). QC parameters (Z' and S/B) and IC_{50} values of pharmacological controls (actinonin and NFF449) were calculated at 30, 60, and 90 min of the reaction time. The meprin α assay displayed the best S/B values after 90 min of reaction time using 1.3 nM enzyme; however, the reaction progress curve was not linear at the 90 min time point (Fig. 3A). This suggested that while longer reaction times and higher than 1.3 nM enzyme concentration may lead to somewhat better S/B values, the assay sensitivity may suffer due to a non-linear relationship between signal and proteolysis inhibition. Therefore, to ensure optimal assay sensitivity, we chose 60 min reaction end point and 1.3 nM meprin α as final assay conditions for the primary HTS campaign.

Preprints (www.preprints.org) | NOT PEER-REVIEWED | Posted: 14 December 2020 doi:10.20944/preprints202012.0354.v1

The meprin β assay progress curve was hyperbolic rather than linear at 0.05 nM and 0.025 nM enzyme; therefore, we chose 0.0125 nM enzyme concentration where assay linearity was demonstrated (Fig. 3B). Z' and S/B values were acceptable at 60 min reaction end point (0.86 and 2.6, respectively). IC_{50} values of NFF449 were not significantly affected by the variations of reaction length and meprin β concentrations.

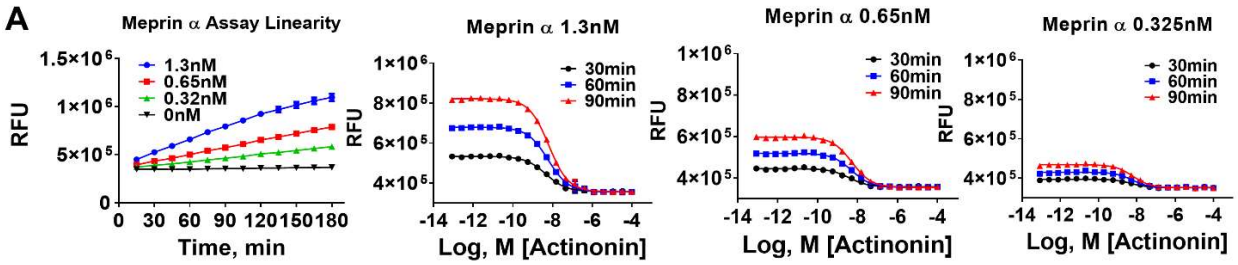

Time, min	1.3nM S/B	1.3nM Z'	1.3nM Actinonin IC_{50}, nM	0.65nM S/B	0.65nM Z'	0.65nM Actinonin IC_{50}, nM	0.32nM S/B	0.32nM Z'	0.32nM Actinonin IC_{50}, nM
30	1.50	0.70	4.84	1.24	0.51	4.11	1.11	0.19	5.18
60	1.91	0.77	5.94	1.44	0.67	4.99	1.21	0.50	5.54
90	2.28	0.80	6.33	1.64	0.75	5.20	1.32	0.62	5.83

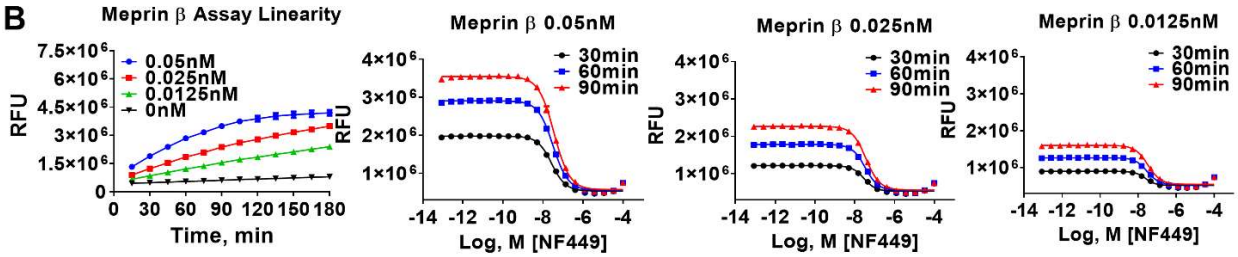

Time, min	0.05nM S/B	0.05nM Z'	0.05nM NF449 IC_{50}, nM	0.025nM S/B	0.025nM Z'	0.025nM NF449 IC_{50}, nM	0.0125nM S/B	0.0125nM Z'	0.0125nM NF449 IC_{50}, nM
30	4.12	0.85	29.60	2.68	0.81	31.04	1.92	0.80	25.22
60	5.75	0.88	34.63	3.73	0.87	36.22	2.56	0.86	30.36
90	6.68	0.89	39.38	4.50	0.88	39.22	3.08	0.88	33.94

Figure 3. Enzyme concentration and time of reaction optimization experiments in 1,536 wpf. (A) Meprin α 1,536 wpf assay optimization study. (B) Meprin β 1,536 wpf assay optimization study. Experiments repeated twice, n=4. S/B – signal-to-basal ratio.

Next, we performed substrate optimization to achieve balanced assay conditions defined as $[S]/K_M = 1$ [12]. In order to do that, we first determined kinetic parameters of proteolysis of meprin α and

Preprints (www.preprints.org) | NOT PEER-REVIEWED | Posted: 14 December 2020 doi:10.20944/preprints202012.0354.v1

meprin β substrates by the respective enzymes (Fig. 4A and B). Meprin α and meprin β proteolysis exhibited similar K_M values (2.4 ± 0.3 μM and 2.7 ± 0.7 μM, respectively) suggesting the need for optimization of both assays' substrate concentration. Meprin β exhibited >20-fold faster turnover of its substrate than meprin α (6.4 ± 0.06 s^{-1} versus 0.29 ± 0.06 s^{-1}, respectively) which is consistent with >100-fold difference in enzyme concentrations for meprin α and meprin β assays (1.3 nM versus 0.0125 nM, respectively). To optimize substrate concentrations, both assays were run for 90 min at three different substrate concentrations (10, 5, and 2.5 μM) which included the concentration at which the assays were recapitulated in 1,536 wpf (10 μM for both meprin α and meprin β) and the concentration approximating $[S]/K_M = 1$ condition (2.5 μM). Enzyme concentrations were fixed at 1.3 nM for meprin α and 0.0125 nM for meprin β. QC parameters (Z' and S/B) and IC_{50} values of pharmacological controls (actinonin and NFF449) were calculated at 40, 60, and 90 min of the reaction time (Fig. 4C and D). 2.5 μM substrate condition resulted in increased apparent potency of pharmacological controls for both assays (2-fold for actinonin in the meprin α assay and 3-fold for NFF449 in the meprin β assay). This suggested that 2.5 μM substrate concentrations result in greater assay sensitivity. Assay QC parameters (S/B and Z') at 2.5 μM substrate concentrations did not differ significantly from assays run at 10 μM substrate concentrations; therefore, we chose 2.5 μM substrate concentrations as a final assay condition.

Preprints (www.preprints.org) | NOT PEER-REVIEWED | Posted: 14 December 2020 doi:10.20944/preprints202012.0354.v1

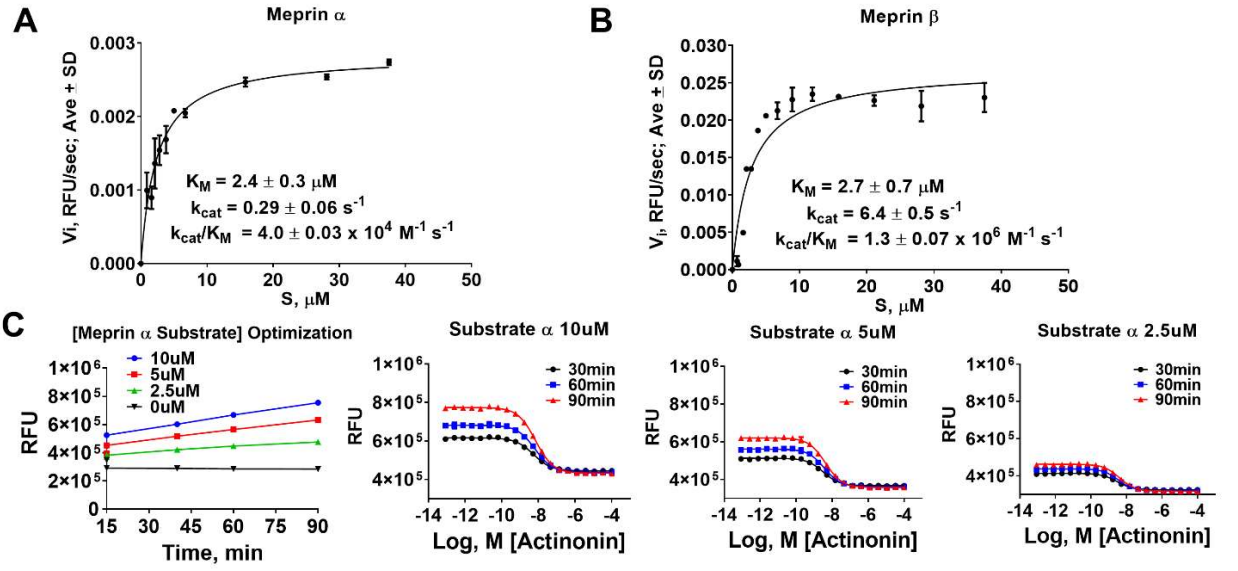

Time, min	10uM			5uM			2.5uM		
	S/B	Z'	Actinonin IC_{50}, nM	S/B	Z'	Actinonin IC_{50}, nM	S/B	Z'	Actinonin IC_{50}, nM
30	1.50	0.80	5.40	1.40	0.83	3.20	1.40	0.82	3.00
60	1.60	0.92	6.40	1.60	0.88	3.70	1.50	0.89	3.40
90	1.90	0.85	6.90	1.90	0.93	4.10	1.60	0.90	4.00

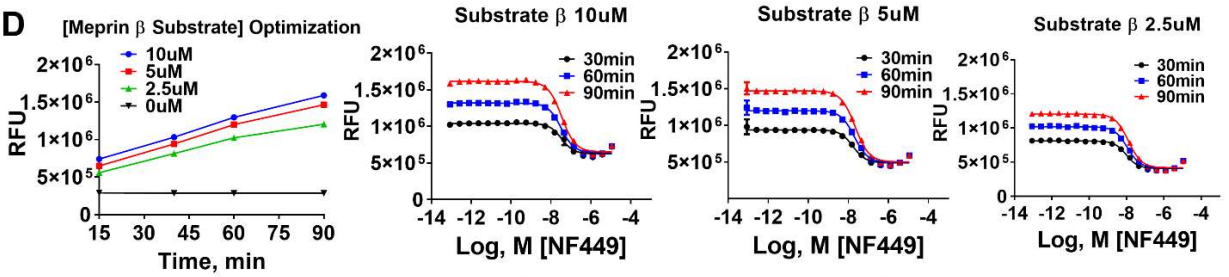

Time, min	10uM			5uM			2.5uM		
	S/B	Z'	NF449 IC_{50}, nM	S/B	Z'	NF449 IC_{50}, nM	S/B	Z'	NF449 IC_{50}, nM
30	2.00	0.87	34.00	2.30	0.89	17.00	2.40	0.89	10.00
60	2.40	0.92	32.00	3.00	0.94	20.00	3.00	0.91	11.00
90	3.00	0.93	34.00	3.60	0.96	22.00	3.60	0.92	13.00

Figure 4. Substrate concentration optimization experiments in 1,536 wpf. Results of kinetic studies of (A) meprin α and (B) meprin β hydrolysis of respective substrates. (C) Meprin α 1,536 wpf assay optimization study. (D) Meprin β 1,536 wpf assay optimization study. Experiments repeated twice, n=4.

Preprints (www.preprints.org) | NOT PEER-REVIEWED | Posted: 14 December 2020 doi:10.20944/preprints202012.0354.v1

Online Robotic Pilot Study. To ascertain the readiness of the assays for large-scale screening effort, a small pilot screen was conducted using online robotics. Overall, ~39,000 compounds were tested using 31 assay plates in both meprin α and meprin β assays. Both assays performed well on the Kalypsys robotic system, as the meprin α assay average Z' and S/B were 0.88 ± 0.03 and 2.9 ± 0.07, respectively, while the meprin β assay average Z' and S/B were 0.91 ± 0.03 and 4.5 ± 0.17, respectively. 169 and 260 hits were identified in the meprin α and meprin β assays, respectively, which constituted 0.43% and 0.67% hit rates, respectively. After removal of duplicates, Venn analysis showed that 37 compounds inhibited both meprins, while there were 129 compounds selectively inhibiting meprin α and 220 compounds selectively inhibiting meprin β, suggesting that selective probes for both enzymes can be discovered. This also suggested that both assays are ready for large scale effort.

Primary HTS Campaign. Primary HTS campaigns were conducted using The Scripps Research Institute proprietary library of 649,570 compounds using both meprin α and meprin β assays [13]. Overall, 522 plates were used for each assay with excellent QC parameters (average Z' = 0.86 ± 0.04 and average S/B = 2.8 ± 0.09 for meprin α assay and average Z' = 0.88 ± 0.03 and average S/B = 4.4 ± 0.27 for meprin β assay). IC_{50} values of control compounds were reproducible with literature and our preliminary experiments (meprin α actinonin IC_{50} = 2.9 ± 0.12 nM, n=11 plates; meprin β NF449 IC_{50} = 10.4 ± 0.85 nM, n=11 plates). Using hit cutoffs derived from the average and 3 standard deviations of the activity of all samples tested which were 10.76% and 14.33% for the meprin α and meprin β assays, 5,064 and 4,929 hits were identified which constituted hit rates of 0.78% and 0.76%, respectively. It was noted that the majority of meprin α hits exhibited % inhibition close to the hit cutoff, whereas meprin β hits were distributed evenly in the range of 20-100% inhibition (Fig. 5A and B).

 doi:10.20944/preprints202012.0354.v1

After removal of a handful of duplicates, Venn analysis showed that 1,416 compounds inhibited both meprins, while there were 3,632 compounds selectively inhibiting meprin α and 3,470 compounds selectively inhibiting meprin β (Fig. 5C). Correlational analysis showed 48 and 39 compounds selectively inhibiting meprin α and meprin β, respectively, with %inhibition ≥ 50 (Fig. 5D).

Preprints (www.preprints.org) | NOT PEER-REVIEWED | Posted: 14 December 2020 doi:10.20944/preprints202012.0354.v1

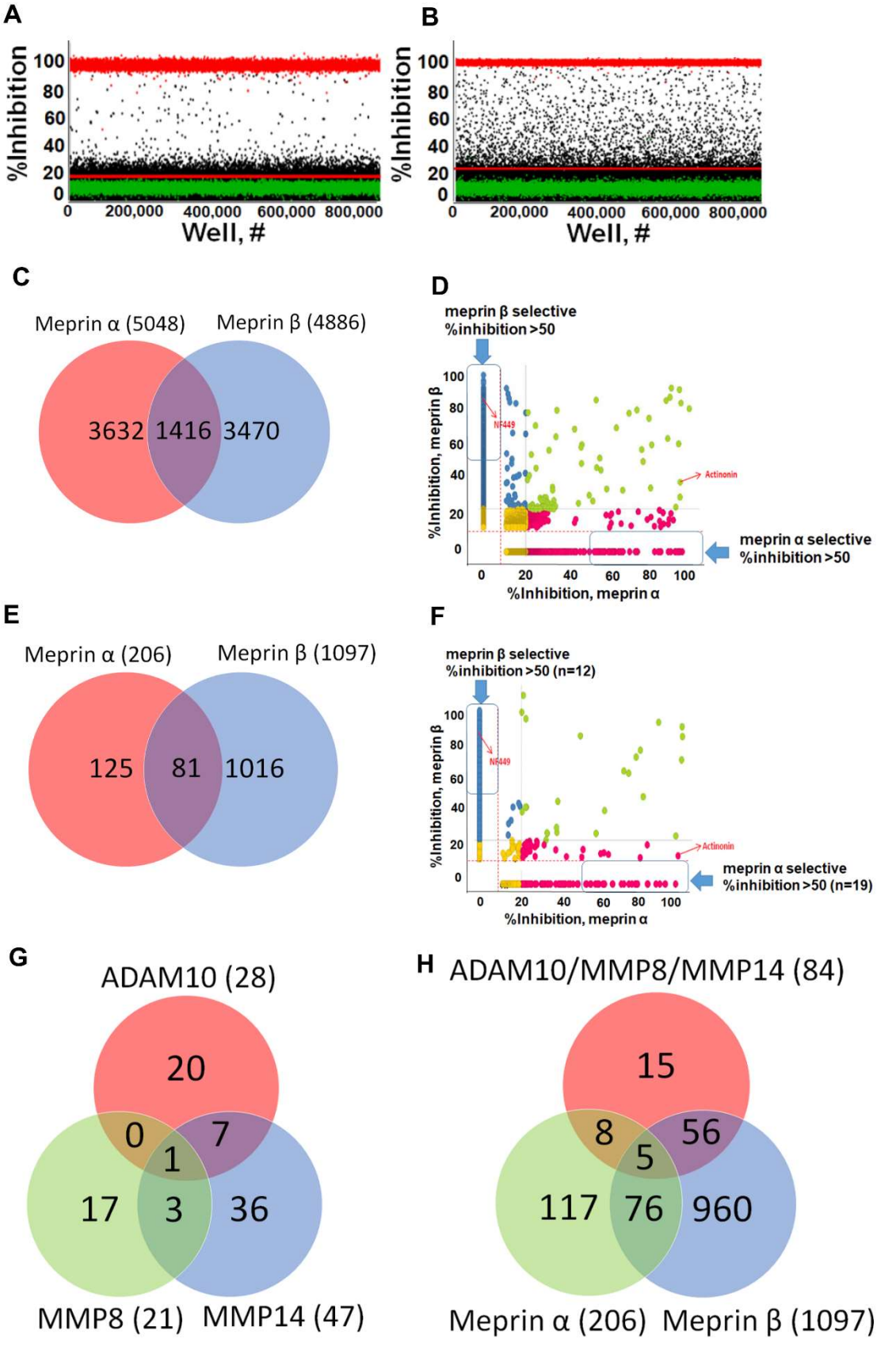

Preprints (www.preprints.org) | NOT PEER-REVIEWED | Posted: 14 December 2020 doi:10.20944/preprints202012.0354.v1

Figure 5. Primary uHTS campaigns. Scatter plots of (A) meprin α and (B) meprin β primary campaigns. Overall, >650,000 compounds were screened in singlicate against each target. (C) Venn diagram of meprin α and meprin β uHTS hits shows 1,416 non-selective hits, 3,632 meprin α and 3,470 meprin β nominally selective hits. (D) Correlation plot of meprin α and meprin β actives demonstrates distribution of hits. (E) Venn diagram of meprin α and meprin β confirmation assays shows confirmed 81 confirmed non-selective hits, 125 meprin α and 1,016 meprin β confirmed selective hits. Each confirmation assay was performed in triplicate. (F) Correlation plot of meprin α and meprin β actives demonstrates distribution of hits. (G) Venn diagram of meprin α and β hits screen against the counter targets MMP-8, MMP-14, and ADAM10. 84 meprin actives inhibited one of three counter targets. (H) Venn diagram of meprin α and β hits versus three combined counter targets. 117 compounds selectively inhibited meprin α while 960 compounds selectively inhibited meprin β.

Hit confirmation and prioritization. For the confirmation assays all compounds that inhibited either meprin with >20% inhibition were selected. Confirmation assays were done at a single concentration point in triplicate. Out of 2,378 total compounds tested in confirmation assays, only 206 confirmed activity against meprin α and 1,097 confirmed activity against meprin β constituting 8.7% and 46.1% confirmation rate for meprin α and meprin β, respectively. The low confirmation rate for meprin α was not unexpected due to the majority of meprin α hits from the primary campaign being close to the hit cutoff (Fig. 5A).

Venn analysis showed that 81 compounds inhibited both meprins, while there were 125 compounds selectively inhibiting meprin α and 1,016 compounds selectively inhibiting meprin β (Fig. 5E). Correlational analysis showed 19 and 12 compounds selectively inhibiting meprin α and β, respectively, with ≥50% inhibition (Fig. 5F). Overall, 827 compounds exhibited >20% inhibition.

It was also noted that the majority of the most active hits for each enzyme were potential Zn-binders due to the presence of hydroxamate and reverse hydroxamate moieties. Compounds acting via Zn binding may be undesirable due to clinical trial failures observed previously based on a lack of selectivity, toxicity, and metabolic instability. To prioritize selectivity, we introduced additional

Preprints (www.preprints.org) | NOT PEER-REVIEWED | Posted: 14 December 2020 doi:10.20944/preprints202012.0354.v1

assays to help with triaging the compounds to ascertain that we are not biasing for non-selective compounds. We utilized ADAM10, MMP-8, and MMP-14 as the most relevant counter targets. The counter screens were conducted in triplicate using the same 2,378 compounds that were tested in confirmation assays.

Venn analysis showed that 84 meprin actives inhibited at least one counter target (Fig. 5G), while there were 117 compounds selectively inhibiting meprin α and 960 compounds selectively inhibiting meprin β (Fig. 5H) and 14 and 75 compounds selectively inhibiting meprin α and meprin β, respectively, with ≥50% inhibition. Cheminformatics analysis of the Scripps HTS assay database containing hundreds of biological assay results showed that 660 out of 1,237 confirmed hits were not promiscuous; meaning they hit in less than 5 other assays. Out of these 660 compounds 536 were meprin α active and 195 were meprin β active. Medicinal chemistry triage suggested that 289 compounds out of 536 meprin α actives were tractable, while out of 195 meprin β actives 180 were tractable, which constitutes 469 total tractable compounds. Removal of 62 duplicates left us with 407 unique compounds of which 404 were available for concentration response studies. Despite the majority of top actives from the 2,378 primary HTS hits being potential Zn-binders, the hit rate in counter screens was <2.0% (Fig. 5G and H) suggesting low metzincin promiscuity of meprin hits.

We conducted concentration response studies of 404 compounds in meprin α and β assays using 10-point 3:1 serial dilutions starting at the highest concentration of 17.4 μM in triplicate. Out of 404 tested compounds, 13 exhibited IC_{50} values <1 μM and 47 <5 μM in in both meprin α and meprin β assays.

To pick compounds for further characterization and probe development we used a cutoff of IC_{50} values < 10 μM against either meprin and 10-fold selectivity window for meprin α or meprin β.

Preprints (www.preprints.org) | NOT PEER-REVIEWED | Posted: 14 December 2020 doi:10.20944/preprints202012.0354.v1

Additionally, we picked the top selective compounds with IC_{50} values <10 μM that had no apparent Zn-binding moieties. More specifically, we prioritized selective compounds without apparent Zn-binding groups (hydroxamates, carboxylates, etc.). Using these criteria, we selected 46 compounds. Interestingly, the majority (42) were selective for meprin β and only 4 were selective for meprin α. These 46 potentially non-Zn-binding compounds were clustered in 21 distinct scaffolds. The most populated scaffold had 9 members suggesting its amenability to medicinal chemistry.

The second group of compounds was chosen based on selectivity between main target (either meprin α or β) and four other tested metzincins (either meprin α or meprin β, ADAM10, MMP-8, and MMP-14) and potency towards the main target (either meprin α or meprin β) regardless of the presence of Zn binders. These criteria yielded 41 compounds belonging to 17 distinct clusters. Interestingly, the majority (32) were selective for meprin α and only 9 were selective for meprin β, which is the opposite trend from non-Zn-binders.

Hit potency, selectivity, and cytotoxicity. We were able to procure 64 out of 87 selected compounds from commercial sources, which we tested in triplicate, 10-point, 3:1 serial dilution concentration response format starting at the highest concentration of 17.4 μM against both meprin α and meprin β. In addition to meprins, we also tested 64 hits against related metzincins (MMP-2, MMP-3, MMP-8, MMP-9, MMP-10, MMP-14, ADAM10, and ADAM17) to ascertain general non-promiscuity against zinc-dependent proteases.

Table 2. Selectivity testing of meprin α top HTS hits. All units are IC_{50}, μM.

Compound ID	Structure	Meprin α	Meprin β	MMP2	MMP3	MMP8	MMP9	MMP10	MMP14	ADAM17

Preprints (www.preprints.org) | NOT PEER-REVIEWED | Posted: 14 December 2020 doi:10.20944/preprints202012.0354.v1

19847	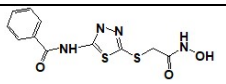	**0.892**	**1.43**	**2.87**	>17	>17	>17	>17	>17	>17
19848	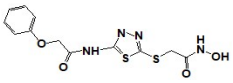	**0.335**	**0.385**	>17	>17	>17	>17	>17	>17	>17
19849	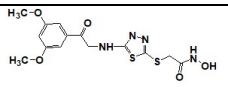	**0.218**	**0.287**	>17	>17	>17	>17	>17	>17	**8.01**
19850	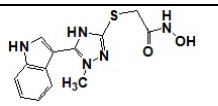	**0.564**	**17**	**17**	>17	>17	>17	>17	>17	**5.03**
19855	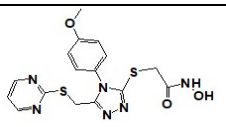	**1.3**	>17	>17	>17	>17	>17	>17	>17	>17
1596857	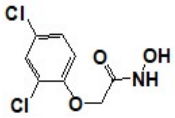	**1.18**	>17	>17	>17	>17	>17	>17	>17	>17
220670	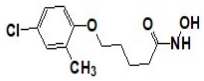	**1.12**	>17	>17	>17	**4.20**	17	>17	>17	>17
162799	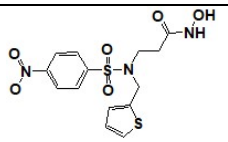	**0.564**	>17	>17	>17	>17	>17	>17	>17	>17
162808	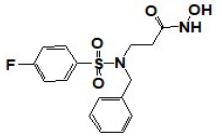	**0.446**	>17	17	>17	>17	>17	>17	>17	>17

The top nine compounds exhibited IC_{50} values ≤1 μM against meprin α (Table 2). Examination of structures of meprin α top hits revealed that they fall into four groups (Fig. 6), thiadiazole-hydroxyacetamides (SR19849, SR19848, SR19847), triazole-hydroxyacetamides (SR19850, SR19855), sulfonamide-hydroxypropanamides (SR162808, SR162799), and phenoxy-hydroxyacetamides (SR1220670, SR1596857). SR162808 was the most potent and selective

Preprints (www.preprints.org) | NOT PEER-REVIEWED | Posted: 14 December 2020 doi:10.20944/preprints202012.0354.v1

inhibitor of meprin α with an IC_{50} value of 0.446 μM and >30-fold selectivity against meprin β and other tested metzincins (Table 2). Both sulfonamide-hydroxypropanamides (SR162808 and SR162799) exhibited sub-micromolar IC_{50} values for meprin α inhibition and >30-fold selectivity against meprin β and other tested metzincins.

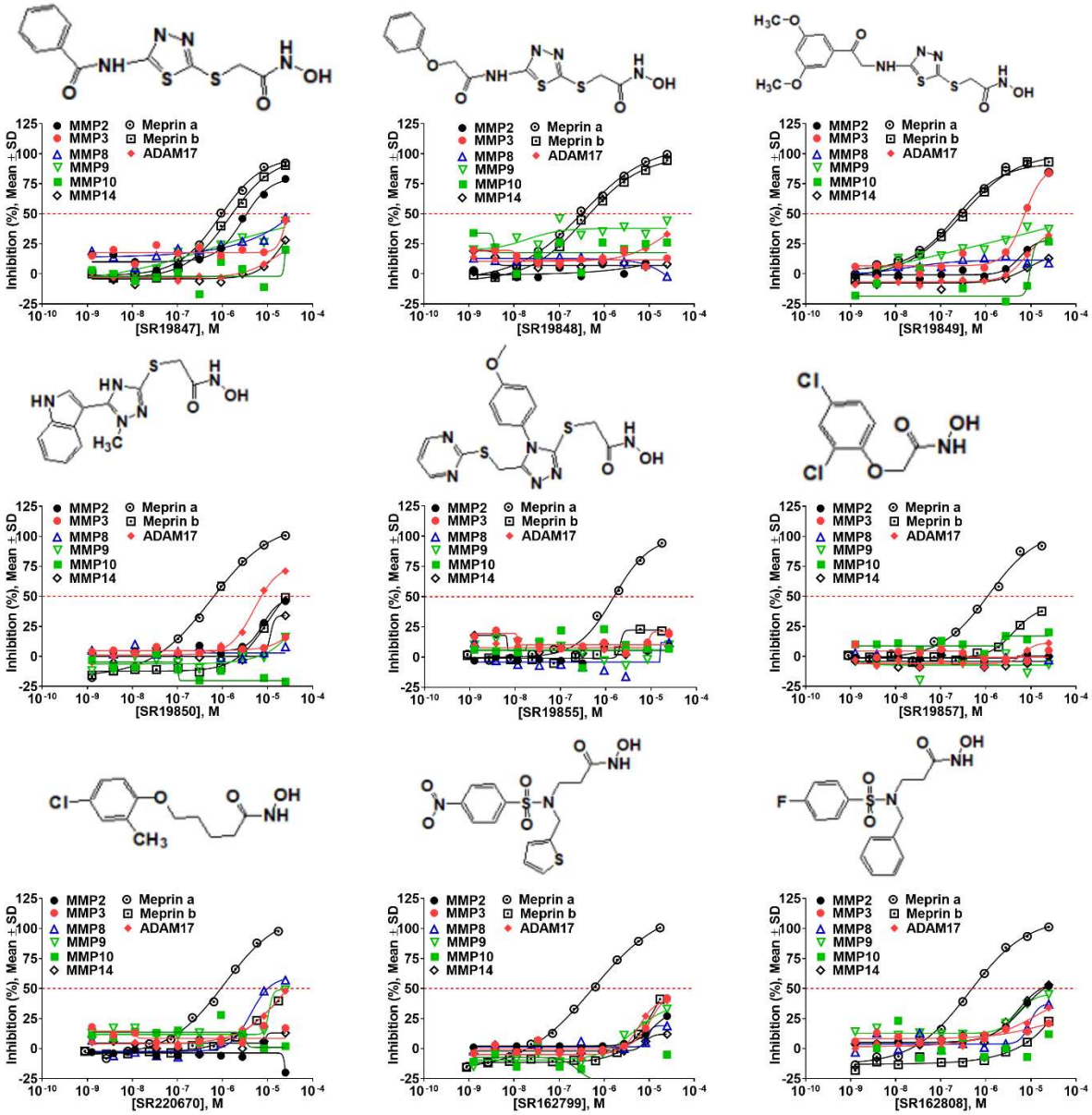

Preprints (www.preprints.org) | NOT PEER-REVIEWED | Posted: 14 December 2020 doi:10.20944/preprints202012.0354.v1

Figure 6. Results of concentration response studies of top potent and selective meprin α inhibitors.

The top meprin β inhibitors belonged to two structural families (Fig. 7 and Table 3), isobutyryl-tetrahydronaphthalen-amides (SR910128, SR910130, and SR910140) and nitrofuran-containing compounds (SR207820 and SR412882). Compound SR355996 was the only representative of the bis-nitrobenzoic acid scaffold.

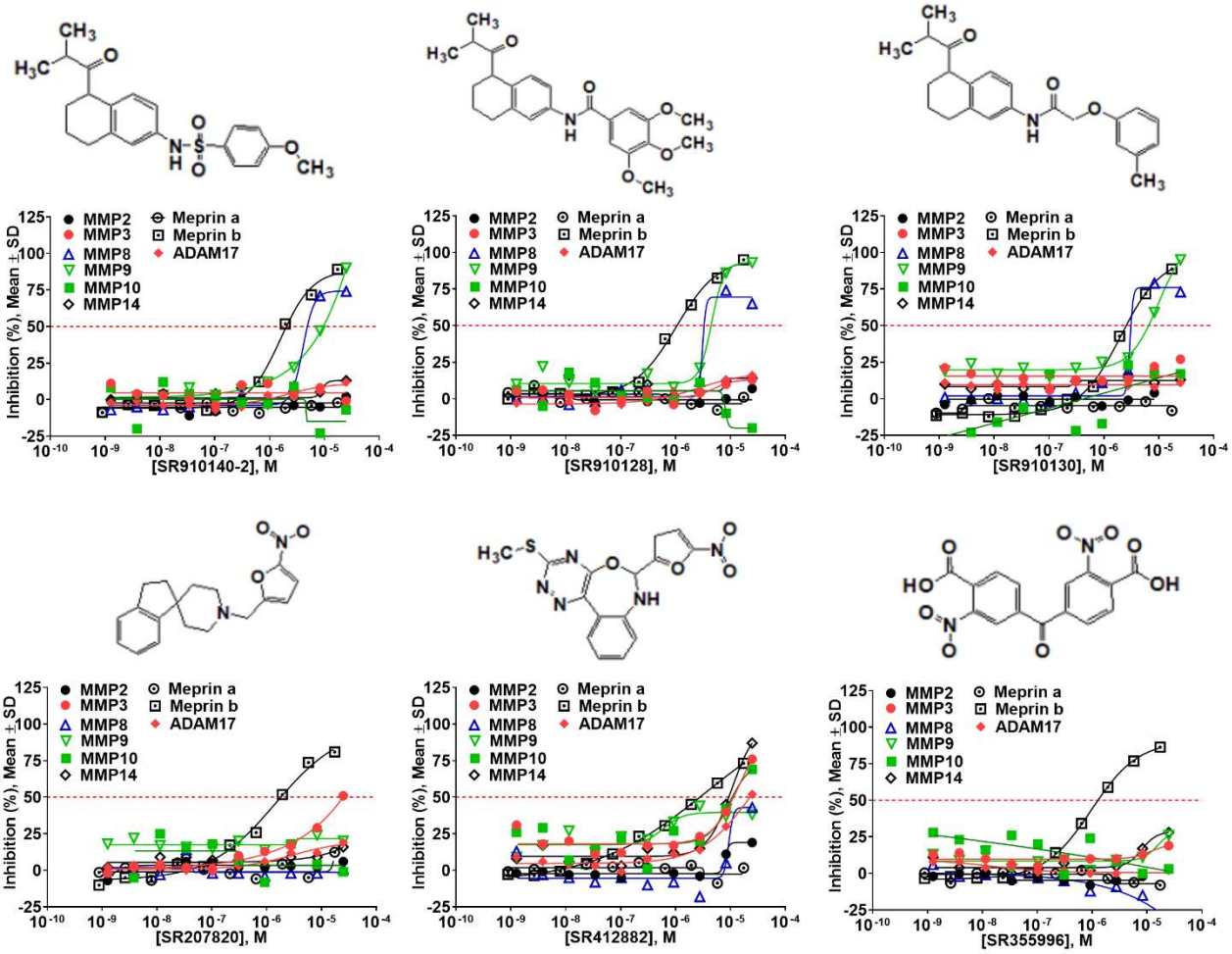

Figure 7. Results of concentration response studies of top potent and selective meprin β inhibitors.

Preprints (www.preprints.org) | NOT PEER-REVIEWED | Posted: 14 December 2020 doi:10.20944/preprints202012.0354.v1

Table 3. Selectivity testing of meprin β top HTS hits. All units are IC_{50}, μM.

Compound ID	Structure	Meprin α	Meprin β	MMP-2	MMP-3	MMP-8	MMP-9	MMP-10	MMP-14	ADAM17
SR207820	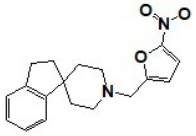	>17	**1.5**	>17	17	>17	>17	>17	>17	>17
SR412882	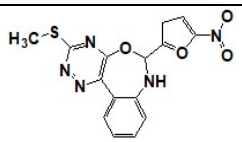	>17	**3.5**	>17	**15**	>17	>17	**9.7**	**10.5**	**17**
SR910128	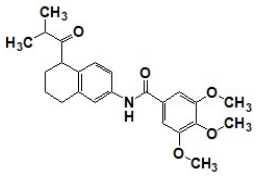	>17	**1.0**	>17	>17	**3.1**	**4.5**	>17	>17	>17
SR910130	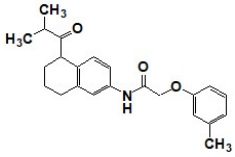	>17	**2.0**	>17	>17	**3.0**	**9.9**	>17	>17	>17
SR910140	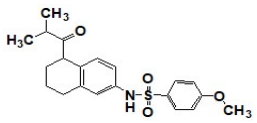	>17	**1.6**	>17	>17	**4.0**	**10**	>17	>17	>17
SR355996	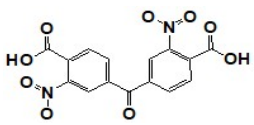	>17	**0.97**	>17	>17	>17	17	>17	>17	>17

We also tested representative compounds from each scaffold for effects on skin fibroblast and melanocyte viability to ascertain cytotoxicity towards various skin cell types. Overall, hits showed either none or very little effect on cell viability (Fig. 8) suggesting a lack of general cytotoxicity and amenability of hit chemotypes for the development into *in vitro* probe for biological studies.

Preprints (www.preprints.org) | NOT PEER-REVIEWED | Posted: 14 December 2020 doi:10.20944/preprints202012.0354.v1

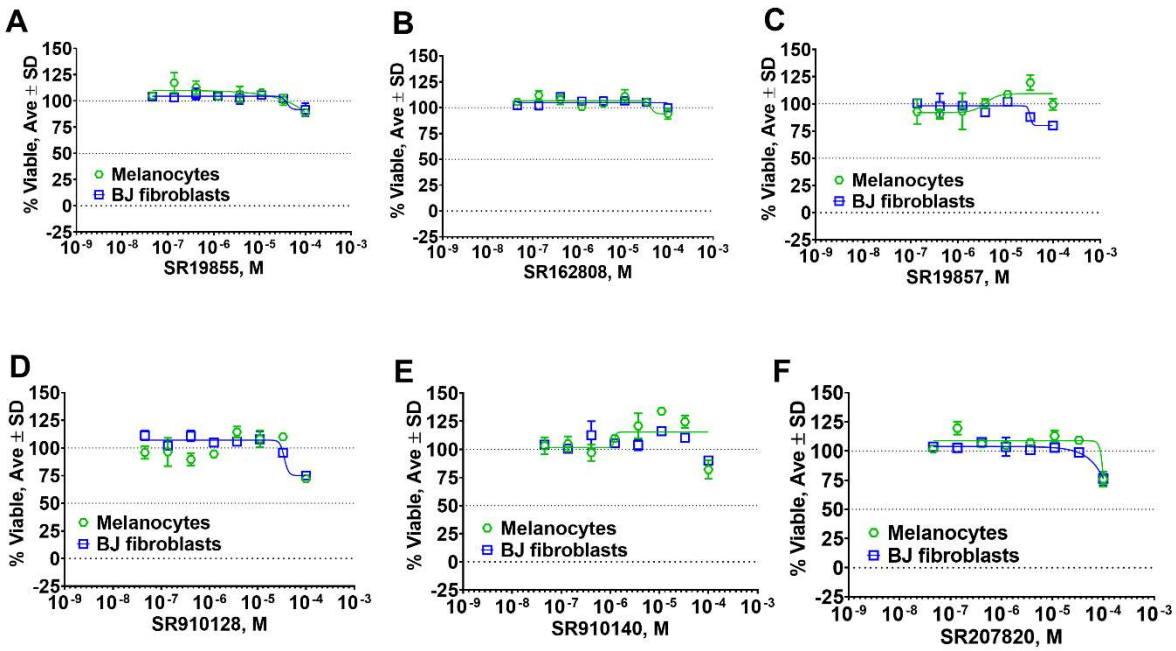

Figure 8. Results of cytotoxicity studies of representative meprin α and meprin β inhibitors. (A-C) Meprin α inhibitors. (D-F) Meprin β inhibitors.

DISCUSSSION

As the result of the uHTS effort we discovered and characterized several novel scaffolds with activity against meprin α and meprin β. All top selective meprin α HTS hits contain a hydroxamate moiety, whereas meprin β hits lack one. Based on the presence of the hydroxamate moiety in meprin α inhibitors it is likely that they act *via* binding of the active site zinc atom as was demonstrated for numerous other metzincins. Tan *et al*., [10] proposed the interaction model whereby the hydroxamic moiety of an analog of compounds **10d** and **10e** (Fig. 1) binds zinc and carboxylate moieties interact with residues of the S_1 and S_1' subsites. Based on this model, the selectivity of **10d** and **10e** is derived from differences between meprin α and meprin β S_1 and S_1' subsites. Both **10d** and **10e** structures are symmetric with a central hydroxamate moiety connected *via* propyl linkers to either terminal benzodioxanes or benzodioxols. Our HTS hits are unlikely to interact

Preprints (www.preprints.org) | NOT PEER-REVIEWED | Posted: 14 December 2020 doi:10.20944/preprints202012.0354.v1

with both subsites as the hydroxamate is terminal in all cases. Similar to **10d** and **10e**, most of the hits (Table 2) have at least one other electronegative moiety in addition to the hydroxamate that could be interacting with positively charged residues in either subsite of meprin α. However, only 5 (SR19855, SR1596857, SR220670, SR162799, and SR162808) out of 9 hits show selectivity for meprin α suggesting that additional interactions may be responsible for selectivity against meprin β.

The most selective and potent meprin α HTS hit, SR162808, exhibited more than 30-fold selectivity against meprin β and other metzincins (Table 2) and no cytotoxicity (Fig. 8b). For comparison, **10d** and **10e** exhibit 18-fold and 19-fold selectivity, respectively (Table 4). Unfortunately, nothing has been reported about their effects on cell viability. For *in vivo* probe or drug lead development a significant selectivity and toxicity window are extremely important; therefore, SR162808 represents a good starting point for a medicinal chemistry optimization effort. In conclusion, an HTS campaign lead to the discovery of 5 selective meprin α hits belonging to three different chemotypes: triazole-hydroxyacetamides (SR19855), sulfonamide-hydroxypropanamides (SR162808 and SR162799), and phenoxy-hydroxyacetamides (SR1220670 and SR1596857). The chemical diversity of the HTS hits, a good metzincin selectivity profile, and low cytotoxicity suggest that these hits can be developed into more potent compounds for *in vivo* studies.

Table 4. Comparison of SR19855 and compounds 10d and 10e from [10]. All units are IC_{50}, μM

ID	Meprin α	Meprin β	Selectivity Fold
SR162808	0.30	>17	38
10d	0.16	2.95	18
10e	0.40	7.59	19

Preprints (www.preprints.org) | NOT PEER-REVIEWED | Posted: 14 December 2020 doi:10.20944/preprints202012.0354.v1

MATERIALS AND METHODS

Reagents. MMP-1, MMP-2, MMP-8, MMP-9, MMP-10, MMP-13, MMP-14, ADAM10, ADAM17 and Mca-KPLGL-Dpa-AR-NH2 fluorogenic peptide substrate were purchased from R&D Systems (cat # 901-MP, 902-MP, 908-MP, 911-MP, 910-MP, 511-MM, 918-MP, 936-AD, 930-ADB, and ES010, respectively). All common chemicals were purchased from Sigma. NFF449 was purchased from Tocris (cat# 1391) and actinonin was from Sigma-Aldrich (cat# 01809).

HTS substrate synthesis. Meprin α and meprin β substrates ((Mca)-YVADAPK-(K-ε-Dnp) and (Mca)-EDEDED-(K-ε-Dnp), respectively) [14] were synthesized utilizing Fmoc solid-phase methodology on a peptide synthesizer. All peptides were synthesized as C-terminal amides to prevent diketopiperazine formation [15]. Cleavage and side-chain de-protection of peptide-resins was for at least 2 h using thioanisole-water-TFA (5:5:90). The substrates were purified and characterized by preparative RP HPLC and characterized by MALDI-TOF MS and analytical RP HPLC.

Meprins expression protocol. Recombinant human meprin α and meprin β were expressed using the Bac-to-Bac expression system (Gibco Life Technologies, Paisley, UK) as described [16-18]. Media and supplements were obtained from Gibco Life Technologies. Recombinant Baculoviruses were amplified in adherently growing *Spodoptera frugiperda* (*Sf*)9 insect cells at 27°C in Grace's insect medium supplemented with 10% fetal bovine serum, 50 units/mL penicillin, and 50 µg/mL streptomycin. Protein expression was performed in 500 mL suspension cultures of BTI-TN-5B1-4 insect cells growing in Express Five SFM supplemented with 4 mM glutamine, 50 units/mL penicillin, and 50 µg/mL streptomycin in Fernbach-flasks using a Multitron orbital shaker

Preprints (www.preprints.org) | NOT PEER-REVIEWED | Posted: 14 December 2020 doi:10.20944/preprints202012.0354.v1

(INFORS AG, Bottmingen, Switzerland). Cells were infected at a density of 2×10^6 cells/mL with an amplified viral stock at a MOI of ~10. Protein expression was stopped after 72 h, and recombinant meprins were further purified from the media by ammonium sulfate precipitation (60% saturation) and affinity chromatography (Streptactin for Strep-tagged meprin α and Ni-NTA for His-tagged meprin β). Meprins were activated by trypsin, which was removed afterwards by affinity chromatography using a column containing immobilized chicken ovomucoid, a trypsin inhibitor.

Meprin α and meprin β assays in 384 well plate. Both assays followed the same general protocol [7]. 5 µL of 2x enzyme solution (2.6 and 0.1 nM for meprin α and meprin β, respectively) in assay buffer (50 mM Hepes, 0.01% Brij-35, pH 7.5) were added to solid bottom black 384 low volume plates (Nunc, cat# 264705). Next, 75 nL of test compounds or pharmacological control (actinonin or NFF449) were added to corresponding wells using a 384-pin tool device (V&P Scientific, San Diego). After 30 min incubation at RT, the reactions were started by addition of 5 µL of 2x solutions of substrates (20 µM, mepin α substrate Mca-YVADAPK-K(Dnp) or meprin β substrate Mca-EDEDED-K(Dnp)). Reactions were incubated at RT for 1 h, after which the fluorescence was measured using the Synergy H4 multimode microplate reader (Biotek Instruments) ($\lambda_{excitation}$ = 324 nm, $\lambda_{emission}$ = 390 nm).

Three parameters were calculated on a per-plate basis: (a) the signal-to-background ratio (S/B); (b) the coefficient for variation [CV; CV = (standard deviation/mean) x 100)] for all compound test wells; and (c) the Z- or Z'-factor [11]. Z takes into account the effect of test compounds on the assay window, while Z' is based on controls.

Determination of kinetic parameters of meprin α and meprin β mediated proteolysis of their respective substrates. Substrate stock solutions were prepared at various concentrations in HTS

Preprints (www.preprints.org) | NOT PEER-REVIEWED | Posted: 14 December 2020 doi:10.20944/preprints202012.0354.v1

assay buffer (50 mM Hepes, 0.01% Brij-35, pH 7.5). Assays were conducted by incubating a range of substrate concentrations (2–50 μM) with various meprin concentrations at 25 °C. Fluorescence was measured on a multimode microplate reader Synergy H1 (Biotek Instruments, Winooski, VT) using $\lambda_{excitation}$ = 324 nm and $\lambda_{emission}$ = 393 nm. Rates of hydrolysis were obtained from plots of fluorescence versus time, using data points from only the linear portion of the hydrolysis curve. The slope from these plots was divided by the fluorescence change corresponding to complete hydrolysis and then multiplied by the substrate concentration to obtain rates of hydrolysis in units of μM/s. Kinetic parameters were calculated by non-linear regression analysis using the GraphPad Prism 8.0 suite of programs.

Meprin α and meprin β assays in 1,536 well plate format. Both assays followed the same general protocol. 2 μL of 2x enzyme solution (1.3 and 0.0125 nM for meprin α and meprin β, respectively) in assay buffer (50 mM Hepes, 0.01% Brij-35, pH 7.5) were added to solid bottom black 1,536 low volume plates (Corning cat# 7261). Next, 30 nL of test compounds or pharmacological control (actinonin or NFF449) were added to corresponding wells using a 1,536 pin tool device (V&P Scientific, San Diego). After 30 min incubation at RT, the reactions were started by addition of 2 μL of 2x solutions of substrates (20 μM, meprin α substrate Mca-YVADAPK-K(Dnp) or meprin β substrate Mca-EDEDED-K(Dnp)). Reactions were incubated at RT for 1 h, after which the fluorescence was measured using the Viewlux multimode microplate reader (Perkin Elmer) ($\lambda_{excitation}$ = 324 nm, $\lambda_{emission}$ = 390 nm).

Three parameters were calculated on a per-plate basis: (a) the signal-to-background ratio (S/B); (b) the coefficient for variation [CV; CV = (standard deviation/mean) x 100)] for all compound test wells; and (c) the Z- or Z'-factor [11]. Z takes into account the effect of test compounds on the assay window, while Z' is based on controls.

Preprints (www.preprints.org) | NOT PEER-REVIEWED | Posted: 14 December 2020 doi:10.20944/preprints202012.0354.v1

uHTS campaign. The miniaturized 1536-well plate format meprin α and meprin β assays were used to screen a collection of approximately 650,000 compounds (The Scripps Research library) on the automated Kalypsys/GNF platform at The Scripps Research Molecular Screening Center (SRMSC, Jupiter, FL, http://hts.florida.scripps.edu/). Both uHTS campaigns were run separately but in a similar manner. Briefly, the first step was the primary screen of all test compounds as singlicates against the meprin α and meprin β target at a final concentration of 7.0 μM. Next, compounds selected as primary hits were cherry-picked and retested in triplicate against the primary screen target and its anti-target (meprin α for the meprin β screening effort, and vice-versa) at a same final concentration of 7.0 μM. The additional counter screen assays against related metzincins (MMP-8, MMP-14, and ADAM10) were performed in triplicate at a final concentration of 7.0 μM. The final step was the titration of selected hits as 10-point, 1:3 serial dilutions in both the target and anti-target assay, starting at a final nominal concentration of 17 μM. For all the aforementioned assays, actinonin and NFF449, for meprin α and meprin β, respectively, at a final concentration of 1 μM, were used as a positive control and reference for 100% inhibition. Wells treated with DMSO only were used as negative controls and 0% inhibition reference. The percent inhibition of each well was then normalized as follows:

%_Inhibition = (RFU_Test_Compound - MedianRFU_Low_Control) / (MedianRFU_High_Control - MedianRFU_Low_Control) * 100

where "Test_Compound" refers to wells containing test compound, "High_Control" is defined as wells treated with either actinonin or NFF449 (n=24) and "Low_Control" as wells containing DMSO only (n=24). All data generated during this effort were uploaded to the SRMSC's institutional screening database (Assay Explorer, Symyx). Sample to background (S/B) ratios, as

Preprints (www.preprints.org) | NOT PEER-REVIEWED | Posted: 14 December 2020 doi:10.20944/preprints202012.0354.v1

well as Z and Z' values, were calculated on a per-plate basis as described [7]. Curve fitting and resulting IC_{50} determinations were performed as previously reported [19].

ADAM10 and ADAM17 assays. Both assays followed the same general protocol. 2.5 µL of 2x enzyme solution (20 nM) in assay buffer (10 mM HEPES, 0.001% Brij-35, pH 7.5) were added to solid bottom black 1536 plates (Greiner, cat# 789075). Next, test compounds and pharmacological controls were added to corresponding wells using a 1536 pin tool device (V&P Scientific, San Diego). After 30 min incubation at RT, the reactions were started by addition of 2.5 µL of 2x solutions of substrate (R&D Systems cat#: ES010, Mca-KPLGL-Dpa-AR-NH_2, 20 µM). Reactions were incubated at RT for 2 h, after which the fluorescence was measured using Perkin Elmer Viewlux multimode microplate imager) ($\lambda_{excitation}$ = 324 nm, $\lambda_{emission}$ = 390 nm). Final concentration of test compounds in assays was 7.0 µM.

MMP assays. All assays followed the same general protocol. 5 µL of 2x enzyme solution (5 nM) in assay buffer (50 mM Tricine, 50mM NaCl, 10mM $CaCl_2$, 0.05% Brij-35, pH 7.5) were added to solid bottom black 384 plates (Nunc, cat# 264705). Next, test compounds and pharmacological controls were added to corresponding wells using a 384-pin tool device (V&P Scientific, San Diego). After 30 min incubation at RT, the reactions were started by addition of 5 µL of 2x solutions of substrate (R&D Systems cat#: ES010, Mca-KPLGL-Dpa-AR-NH_2, 20 µM). Reactions were incubated at RT for 1 h, after which the fluorescence was measured using the Synergy H4 multimode microplate reader (Biotek Instruments) ($\lambda_{excitation}$ = 324 nm, $\lambda_{emission}$ = 390 nm).

Cell toxicity studies. Test compounds were solubilized in 100% DMSO and added to polypropylene 384 well plates (Greiner cat# 781280). 1,250 of BJ skin fibroblasts (ATCC® CRL-2522™) and primary melanocytes (ATCC® PCS-200-013™) were plated in 384-well plates in 8 µL of serum-free media (HybriCare for BT474, EMEM for HEK293). Test compounds and

 doi:10.20944/preprints202012.0354.v1

pharmacological assay control (lapatinib) were prepared as 10-point, 1:3 serial dilutions starting at 10 mM, then added to the cells using the pin tool mounted on the Integra 384. Plates were incubated for 72 h at 37°C, 5% CO_2 and 95% relative humidity. After incubation, 8 µL of CellTiter-Glo® (Promega cat# G7570) was added to each well and incubated for 15 min at room temperature. Luminescence was recorded using a Biotek Synergy H1 multimode microplate reader. Viability was expressed as a percentage relative to wells containing media only (0%) and wells containing cells treated with DMSO only (100%). Three parameters were calculated on a per-plate basis: (a) the signal-to-background ratio (S/B); (b) the coefficient for variation [CV; CV = (standard deviation/mean) x 100)] for all compound test wells; and (c) the Z'-factor. IC_{50} values were calculated by fitting normalized data to sigmoidal log versus response equation utilizing non-linear regression analysis from GraphPad Prizm 8.

AUTHOR INFORMATION

Corresponding Author

*Email: dminond@nova.edu

Abbreviations.

uHTS - ultra-high throughput screening; MMP - matrix metalloprotease; ADAM - a disintegrin and metalloprotease.

Acknowledgements and Funding Sources

This work was supported by the National Institutes of Health (AR066676 and CA249788 to DM). This work was also supported by the Deutsche Forschungsgemeinschaft (DFG) grant SFB877 "Proteolysis as a Regulatory Event in Pathophysiology" (project A9 and A15) (both to C.B.-P.). We thank Pierre Baillargeon and Lina DeLuca (Lead Identification, Scripps Florida) for compound management.

Author Contributions Statement

D.M. designed and oversaw the study, developed HTS assays, performed kinetic studies, performed post-HTS biochemical *in vitro* characterization of hits, wrote the first manuscript draft and prepared figures. JD performed cytotoxicity studies. G.B.F synthesized and purified meprin α and meprin β substrates and edited the manuscript. TB and CW triaged HTS hits via cheminformatics. C.B.P. expressed meprin α and meprin β. SH, LDS and TPS performed uHTS campaign. All authors reviewed the manuscript.

Notes

The authors declare no competing financial interests.

REFERENCES

1. Peters, F.; Becker-Pauly, C., Role of meprin metalloproteases in metastasis and tumor microenvironment. *Cancer Metastasis Rev* **2019,** *38* (3), 347-356.
2. Prox, J.; Arnold, P.; Becker-Pauly, C., Meprin alpha and meprin beta: Procollagen proteinases in health and disease. *Matrix Biol* **2015,** *44-46*, 7-13.
3. Broder, C.; Arnold, P.; Vadon-Le Goff, S.; Konerding, M. A.; Bahr, K.; Muller, S.; Overall, C. M.; Bond, J. S.; Koudelka, T.; Tholey, A.; Hulmes, D. J.; Moali, C.; Becker-Pauly, C., Metalloproteases meprin alpha and meprin beta are C- and N-procollagen proteinases important for collagen assembly and tensile strength. *Proc Natl Acad Sci U S A* **2013,** *110* (35), 14219-24.
4. Becker-Pauly, C.; Pietrzik, C. U., The Metalloprotease Meprin beta Is an Alternative beta-Secretase of APP. *Front Mol Neurosci* **2016,** *9*, 159.

5. Scharfenberg, F.; Armbrust, F.; Marengo, L.; Pietrzik, C.; Becker-Pauly, C., Regulation of the alternative beta-secretase meprin beta by ADAM-mediated shedding. *Cell Mol Life Sci* **2019,** *76* (16), 3193-3206.
6. Kruse, M. N.; Becker, C.; Lottaz, D.; Kohler, D.; Yiallouros, I.; Krell, H. W.; Sterchi, E. E.; Stocker, W., Human meprin alpha and beta homo-oligomers: cleavage of basement membrane proteins and sensitivity to metalloprotease inhibitors. *Biochem J* **2004,** *378* (Pt 2), 383-9.
7. Madoux, F.; Tredup, C.; Spicer, T. P.; Scampavia, L.; Chase, P. S.; Hodder, P. S.; Fields, G. B.; Becker-Pauly, C.; Minond, D., Development of high throughput screening assays and pilot screen for inhibitors of metalloproteases meprin alpha and beta. *Biopolymers* **2014,** *102* (5), 396-406.
8. Ramsbeck, D.; Hamann, A.; Schlenzig, D.; Schilling, S.; Buchholz, M., First insight into structure-activity relationships of selective meprin beta inhibitors. *Bioorg Med Chem Lett* **2017,** *27* (11), 2428-2431.
9. Ramsbeck, D.; Hamann, A.; Richter, G.; Schlenzig, D.; Geissler, S.; Nykiel, V.; Cynis, H.; Schilling, S.; Buchholz, M., Structure-Guided Design, Synthesis, and Characterization of Next-Generation Meprin beta Inhibitors. *J Med Chem* **2018,** *61* (10), 4578-4592.
10. Tan, K.; Jager, C.; Schlenzig, D.; Schilling, S.; Buchholz, M.; Ramsbeck, D., Tertiary-Amine-Based Inhibitors of the Astacin Protease Meprin alpha. *ChemMedChem* **2018,** *13* (16), 1619-1624.
11. Zhang, J. H.; Chung, T. D.; Oldenburg, K. R., A Simple Statistical Parameter for Use in Evaluation and Validation of High Throughput Screening Assays. *J Biomol Screen* **1999,** *4* (2), 67-73.
12. Copeland, R., *Evaluation of enzyme inhibitors in drug discovery*. 1st ed.; John Wiley and Sons: 2005; p 113-117.
13. Baillargeon, P.; Fernandez-Vega, V.; Sridharan, B. P.; Brown, S.; Griffin, P. R.; Rosen, H.; Cravatt, B.; Scampavia, L.; Spicer, T. P., The Scripps Molecular Screening Center and Translational Research Institute. *SLAS Discov* **2019,** *24* (3), 386-397.
14. Broder, C.; Becker-Pauly, C., The metalloproteases meprin alpha and meprin beta: unique enzymes in inflammation, neurodegeneration, cancer and fibrosis. *Biochem J* **2013,** *450* (2), 253-64.
15. Fields, G. B.; Lauer-Fields, J. L.; Liu, R.-q.; Barany, G., Principles and Practice of Solid-Phase Peptide Synthesis. In *Synthetic Peptides: A User's Guide*, 2nd ed.; Grant, G. A., Ed. W.H. Freeman & Co.: New York, 2001; pp 93-219.
16. de Jong, G. I.; Buwalda, B.; Schuurman, T.; Luiten, P. G., Synaptic plasticity in the dentate gyrus of aged rats is altered after chronic nimodipine application. *Brain Res* **1992,** *596* (1-2), 345-8.
17. Becker-Pauly, C.; Howel, M.; Walker, T.; Vlad, A.; Aufenvenne, K.; Oji, V.; Lottaz, D.; Sterchi, E. E.; Debela, M.; Magdolen, V.; Traupe, H.; Stocker, W., The alpha and beta subunits of the metalloprotease meprin are expressed in separate layers of human epidermis, revealing different functions in keratinocyte proliferation and differentiation. *J Invest Dermatol* **2007,** *127* (5), 1115-25.
18. Becker, C.; Kruse, M. N.; Slotty, K. A.; Kohler, D.; Harris, J. R.; Rosmann, S.; Sterchi, E. E.; Stocker, W., Differences in the activation mechanism between the alpha and beta subunits of human meprin. *Biol Chem* **2003,** *384* (5), 825-31.

 doi:10.20944/preprints202012.0354.v1

19. Smith, E.; Chase, P.; Niswender, C. M.; Utley, T. J.; Sheffler, D. J.; Noetzel, M. J.; Lamsal, A.; Wood, M. R.; Conn, P. J.; Lindsley, C. W.; Madoux, F.; Acosta, M.; Scampavia, L.; Spicer, T.; Hodder, P., Application of Parallel Multiparametric Cell-Based FLIPR Detection Assays for the Identification of Modulators of the Muscarinic Acetylcholine Receptor 4 (M4). *J Biomol Screen* **2015,** *20* (7), 858-68.